Quantum walk in stochastic environment

Ben Avnit and Doron Cohen

Department of Physics, Ben-Gurion University of the Negev, Beer-Sheva 84105, Israel

We consider a quantized version of the Sinai-Derrida model for "random walk in random environment." The model is defined in terms of a Lindblad master equation. For a ring geometry (a chain with periodic boundary condition) it features a delocalization-transition as the bias in increased beyond a critical value, indicating that the relaxation becomes underdamped. Counterintuitively, the effective disorder is enhanced due to coherent hopping. We analyze in detail this enhancement and its dependence on the model parameters. The nonmonotonic dependence of the Lindbladian spectrum on the rate of the coherent transitions is highlighted.

I. INTRODUCTION

Sinai has coined the term "random walk in random environment" for a model that describes the stochastic motion of a particle in a 1D lattice [1]. The forward and backward rates $w_x^{\pm}$ of the transitions between sites (indexed by x) are independent random variables. For a biased chain the average ratio w_x^+/w_x^- favors (say) the forward direction. It turns out that for an unbiased infinite chain with arbitrarily small randomness the spreading of the particle becomes subdiffusive. Later Derrida and followers [2–4] have found that nonzero drift velocity is induced if the bias exceeds a critical value or *sliding transition*. Related to that is the *delocalization transition* that has been. discussed by Hatano, Nelson, and followers [5–10]. The latter term refers, in the Sinai-Derrida context, to the transition from overdamped to underdamped *relaxation* for a finite sample with periodic boundary conditions [11–14].

We consider a quantum version of the Sinai-Derrida model. This means that in addition to the stochastic transitions that are described by an appropriate master equation, the particle can also perform coherent hopping between the sites. The hopping frequency c is a free model parameter. Our interest is focused in the regime $c \ll \nu$, where ν is the average rate of the stochastic transitions. Note that in the other extreme ($\nu = 0$) the model features ballistic motion that can be suppressed by an Anderson localization effect (due to quenched disorder) or by Bloch oscillations (if bias is applied).

In Ref. [15] we have introduced a full Ohmic Lindbladian that generates the quantized version of the Sinai-Derrida model. A counterintuitive enhancement of the effective disorder due to coherent hopping has been pointed out but has not been explored. In particular, the most interesting aspect, namely the delocalization transition, has not been discussed. In the present paper we consider a *minimal version* of the full quantized version, omitting some terms that are not essential for the demonstration of the main effects and performing some further simplifications that will be discussed in subsequent sections. Thus, in the absence of coherent hopping ($c = 0$) our minimal model reduces to the Pauli master equation and hence becomes identical to the standard Sinai-Derrida model.

The minimal model that we introduce below is defined by a Lindbladian. It includes a random potential that has dispersion $\sigma_{\mathcal{E}}$ and a random stochastic field that has dispersion σ_f. The parameters that define the model are (ν, c, $\sigma_{\mathcal{E}}$, σ_f) and the bias f. We argue that such Lindbladian reflects an environment that has a characteristic temperature

$$T_{\text{bath}} = (\sigma_f/\sigma_{\mathcal{E}})^{-1}. \tag{1}$$

An associated dimensionless parameter is

$$\eta = \frac{\nu}{2T_{\text{bath}}} = \frac{1}{2}\left(\frac{\sigma_f}{\sigma_{\mathcal{E}}}\right)\nu. \tag{2}$$

Accordingly, there are two "classical" dimensionless parameters and two "quantum" dimensionless parameters that define the model:

$$\text{Dimensionless Parameters} = (f, \sigma_f, \eta, c/\nu). \tag{3}$$

We introduce the stochastic and the quantized models in Secs. II and III, with extra technical details in the Appendix. We further discuss the significance of the model parameters in Sec. IV and provide a regime diagram in Fig. 1. Then we look on the spectrum of the Lindbladian for nondisordered and for disordered ring in Secs. V and VI, respectively. We discuss how the localization of its eigenmodes is affected by c in Sec. VII and highlight some counterintuitive effects. The delocalization threshold is further explained in Sec. VIII. The summary in Sec. VII provides extra background to place the present work in the context of past studies.

II. THE STOCHASTIC MODEL

The standard Sinai-Derrida model is defined in terms of a rate equation for the probabilities p_x to find the particle in site $x = 1, 2, \dots, N$, and we assume periodic boundary conditions. The rate equation is written as follows:

$$\frac{d}{dt}\boldsymbol{p} = \mathcal{W}\boldsymbol{p}, \tag{4}$$

where $\boldsymbol{p} = \{p_x\}$ is a vector and $\mathcal{W}$ is an $N \times N$ matrix. The explicit expression for this matrix is

$$\mathcal{W} = -\sum_x (w_x^+ + w_{x-1}^-)\boldsymbol{Q}_x + \sum_x [w_x^+ \boldsymbol{D}_x + w_x^- \boldsymbol{D}_x^{\dagger}], \tag{5}$$
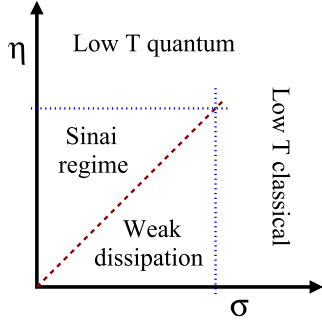
FIG. 1. Regime diagram. The (σ_f, η) regime diagram for the unbiased model. The classical high-temperature condition ($\sigma_f < 1$) implies weak stochastic field. The quantum high-temperature condition ($\eta < 1$) allows us to ignore memory effects. In the Sinai regime, above the dashed line ($\eta > \sigma_f$), the coherent effects are regarded as a perturbation with respect to the dominant stochastic dynamics.

where $\boldsymbol{Q}_x = |x\rangle\langle x|$ and $\boldsymbol{D}_x = |x+1\rangle\langle x|$. The translation operator is $\boldsymbol{D} = \sum_x \boldsymbol{D}_x = e^{-i\boldsymbol{q}}$, where $\boldsymbol{q}$ is the generator of translations. In the absence of disorder the above expression takes the form

$$\mathcal{W} = -(w^+ + w^-)[1 - \cos(\boldsymbol{q})] - i(w^+ - w^-)\sin(\boldsymbol{q}). \quad (6)$$

The rates $w_x^{\pm}$ in the disordered Sinai model are determined by a random stochastic field f_x such that

$$\frac{w_x^-}{w_x^+} \equiv e^{-f_x}. \quad (7)$$

We assume, following Sinai, weak stochastic disordered ($f_x \ll 1$). Consequently, one writes in leading order

$$w_x^{\pm} \equiv \nu_x e^{\pm f_x/2} \approx \left(1 \pm \frac{f_x}{2}\right)\nu_x. \quad (8)$$

Accordingly, ν_x characterizes the strength of the stochastic transitions at a given bond, while f_x reflects their asymmetry.

For the later analysis we write an explicit expression for the $\mathcal{W}$ matrix that holds in leading order with respect to the disorder strength:

$$\mathcal{W} = -\text{diagonal}\left\{(\nu_x + \nu_{x-1}) + \frac{\nu}{2}(f_x - f_{x-1}) + \frac{\nu}{4}f^2\right\}$$
$$+ \text{off-diagonal}\left\{\nu_x e^{\pm f_x/2}\right\}. \quad (9)$$

In the above formula the off-diagonal terms are written without any approximation, because it is more convenient for later discussion. But a clarification is required for the approximations that are involved in the diagonal terms. The term $\nu(f_x - f_{x-1})$ is implied by the replacement of ν_x by its average value ν. The error that is associated with this replacement is of higher order in the disorder strength. The same reasoning applies for the νf^2 term, where the replacement of f_x by its average value f has been performed.

The random independent variables f_x are characterized by an average $f_{\text{bias}} \equiv f$ and by a dispersion σ_f. The spectrum of $\mathcal{W}$ is illustrated in Fig. 2. As f is increased more eigenvalues become complex (see lower panel). The critical value f_c is the value above which complex eigenvalues emerge at the vicinity of $\lambda \sim 0$. This is identified as a *delocalization transition* in the
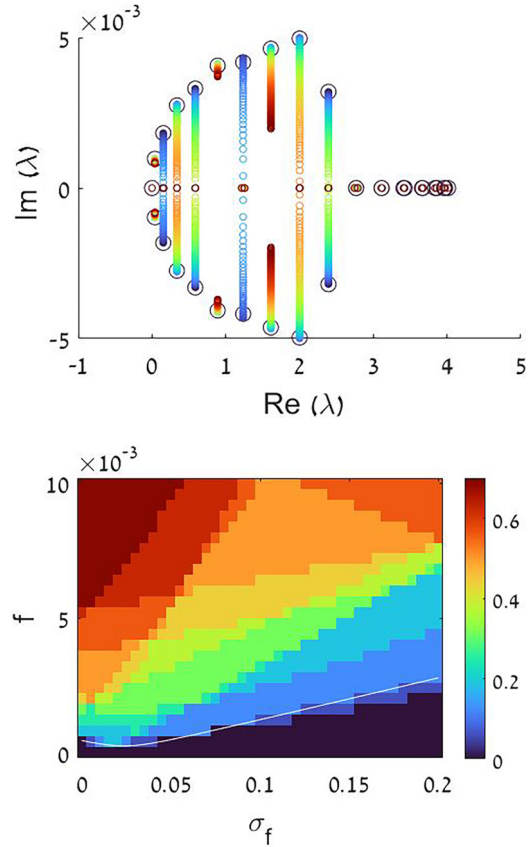

FIG. 2. Delocalization of the eigenmodes. The chain consist of $N = 32$ sites with periodic boundary conditions. The dynamics is described by a rate equation with matrix $\mathcal{W}$. The average transition rate between neighboring sites is $\nu = 1$ and $\sigma_\nu = 0.05$. Upper panel: The spectra of $\mathcal{W}$ for $f = 0.005$. The color code indicates the value of σ. It goes from blue ($\sigma_f = 0$) to red ($\sigma_f = 0.02$). Lower panel: Characterization of the spectrum in a wider range. The axes are σ_f and f. The color code indicates the normalized number N_{cmplx}/N of complex eigenvalues. The solid line indicates the numerically determined critical value f_c above which the eigenvalues at the vicinity of $\lambda = 0$ become complex. For different realizations of the disorder this line is shifted within some range.

sense of Hatano and Nelson [11] and has a subtle relation [11] to the *sliding transition* that has been discussed by Derrida and followers. An estimate for f_c can be obtained by the formula

$$f_c = \tfrac{1}{4}\text{Var}(f_x) = \text{prefactor } \sigma_f^2, \quad (10)$$

where the numerical prefactor depends on the numerical definition of σ_f that may vary depending on the shape (Gaussian/Box) of the distribution. This expression works well for a long chain, while fluctuations in its value are pronounced for short samples.

III. THE QUANTIZED MODEL

The full Ohmic version of the Lindblad equation for an N site chain with periodic boundary conditions can be found in the Appendix. Here we summarize the details of a simplified minimal version that still contains all the essential physics of the problem under study. The master equation for the

evolution of the probability matrix is

$$\frac{d\rho}{dt} = [\mathcal{L}^{(\mathcal{H})} + \mathcal{L}^{(\text{bias})} + \mathcal{L}^{(B)} + \mathcal{L}^{(S)}]\rho. \qquad (11)$$

The Lindblad generators in this equation refer to the coherent Hamiltonian dynamics, to the coherent bias term, to the stochastic environmentally induced transitions between sites (along "*B*onds"), and to optional decoherence due to local baths (at "*S*ites"). The explicit expressions are as follows:

$$\mathcal{L}^{(\mathcal{H})}\rho = -i[\boldsymbol{H}, \rho], \qquad (12)$$

$$\mathcal{L}^{(B)}\rho = -\frac{1}{2}\sum_x (w_x^+ + w_{x-1}^-)[\boldsymbol{Q}_x\rho + \rho\boldsymbol{Q}_x]$$

$$+ \sum_x [w_x^+ \boldsymbol{D}_x^\dagger \rho \boldsymbol{D}_x + w_x^- \boldsymbol{D}_x \rho \boldsymbol{D}_x^\dagger], \qquad (13)$$

$$\mathcal{L}^{(S)}\rho = -\gamma\rho + \sum_x \gamma \boldsymbol{Q}_x \rho \boldsymbol{Q}_x. \qquad (14)$$

The stochastic transition rates are $w_x^\pm$ as in Eq. (8), and the extra on-site decoherence rate is γ. The Hamiltonian incorporates a hopping term and a disordered potential:

$$\mathcal{H} = \frac{c}{2}(\boldsymbol{D} + \boldsymbol{D}^\dagger) + U(\boldsymbol{x}), \qquad (15)$$

where c is the hopping frequency for coherent transitions. The disordered field is

$$\mathcal{E}_x = -[U(x+1) - U(x)]. \qquad (16)$$

If we did not impose periodic boundary conditions, then the bias could have been added using the prescription $U(x) \mapsto U(x) - \mathcal{E}x$, with diagonal matrix elements $i(x_n - x_m)\mathcal{E}_{\text{bias}}$. In order to respect the periodic boundary condition we modify the bias term as follows:

$$\mathcal{L}^{(\text{bias})}(n', m'|n, m) = i\delta_{n',n}\delta_{m',m}\,\mathcal{E}_{\text{bias}}\frac{N}{2\pi}\sin\left[\frac{2\pi}{N}(x_n - x_m)\right]. \qquad (17)$$

This modified version is locally the same as the proper version for an open chain, while for large $(x_n - x_m)$ it can be justified self-consistently for a long closed chain. This modification has no significant numerical implication, because the far off-diagonal terms of the probability matrix for low modes are vanishingly small.

The definition of the local temperature T_x is implied by the Boltzmann ratio Eq. (7), using the substitution

$$f_x \equiv \frac{\mathcal{E}_x}{T_x}. \qquad (18)$$

Recall that we assume, following Sinai, weak stochastic disordered ($f_x \ll 1$), which is equivalent to $\mathcal{E}_x \ll T_x$. This goes well with the observation that the Ohmic approximation is consistent with Boltzmann to leading order in $1/T$ (higher-order terms in the Ohmic master equation vanish only in the classical limit). In the Appendix we explain how Eq. (18) is obtained rigorously from the Ohmic master equation. The free parameters of the Ohmic master equation are ν_x and η_x that correspond to the "noise" intensity and the "friction" coefficient in the common Langevin description. They obey the Einstein relation, namely $T_x = \nu_x/(2\eta_x)$. However, in the

present model the coupling of the bonds to the baths implies that η should be regraded as a "mobility" and not as "friction" coefficient [15].

IV. MODEL PARAMETERS

Physically disorder may arise from the potential, or from the environmental parameters. So we may have randomness in ν_x and/or in η_x and/or in $\mathcal{E}_x$ and/or in γ_x. The Sinai-Derrida physics that we discuss is rather robust and allows flexibility in the choice of the "free" parameters. In the numerical study, the following approach has been adopted with no loss of generality. Given $\sigma_\mathcal{E}$ we generate a realizations of the disordered potential such that

$$U(x) \in [0, \sigma_\mathcal{E}]. \qquad (19)$$

Then we can generate a random $\eta_x \in [0, \sigma_\eta]$ and from it calculate the random stochastic field f_x. In practice we have realized that the numerical results are robust and not affected if we generate the stochastic field independently, namely

$$f_x \in \left[f - \frac{\sigma_f}{2}, f + \frac{\sigma_f}{2}\right] \qquad (20)$$

with

$$\text{Var}(f_x) = \frac{C}{\nu^2}\sigma_\eta^2\,\text{Var}(\mathcal{E}_x). \qquad (21)$$

The latter relation follows from Eq. (24) of Ref. [13], where $C = 8$ for Gaussian disorder. From this relation it follows that the ratio $\sigma_f/\sigma_\mathcal{E}$ is determined by the temperature of the bath. This inspires the practical definition of the characteristic temperature Eq. (1).

A. Resistor network disorder

The essential type of disorder for the discussion of Sinai-Derrida physics is related to the randomness of the stochastic field f_x. As opposed to that, randomness in ν_x is similar to "resistor network disorder." It has significant implications only in extreme circumstances, such that *percolation* becomes an issue [11]. We assume weak disorder, and therefore the probability for disconnected bonds is zero. For the numerical exploration we take

$$\nu_x \in \left[\nu - \frac{\sigma_\nu}{2}, \nu + \frac{\sigma_\nu}{2}\right], \qquad (22)$$

where ν is the average value of ν_x, and $\sigma_\nu \ll \nu$ is assumed.

B. Numerical procedure

Given σ_ν we generate random set of ν_x values for the bonds in accordance with Eq. (22). We set the units of time such that the average value is $\nu = 1$. Given σ_f and f, we generate random realizations of the stochastic field f_x in accordance with Eq. (20), such that $\sum f_x \equiv Nf$ for each realization. Note that the average value f, per realization, is regarded as a control parameter, namely $f_{\text{bias}} \equiv f$. The transition rates $w_x^\pm$ are calculated using Eq. (8). Given T_{bath} we determine $\sigma_\mathcal{E}$ from Eq. (1) and generate a realization of the disordered potential in accordance with Eq. (19). Respectively in Eq. (17) we substitute $\mathcal{E}_{\text{bias}} = T_{\text{bath}}f_{\text{bias}}$.

C. Regime diagram

The (σ_f, η) regime diagram of the unbiased model is displayed in Fig. 1. The assumed hierarchy of energy scales is

$$c, \ \sigma_{\mathcal{E}} \ \ll \ \nu \ \ll \ T_{\text{bath}}. \tag{23}$$

The horizontal axis of the diagram is the strength σ_f of the Sinai disorder that is determined by the ratio between $\sigma_{\mathcal{E}}$ and T_{bath} via Eq. (1). As already pointed out we assume weak stochastic field ($\sigma_f \ll 1$) reflecting that we deal with an Ohmic master equation that corresponds to the traditional Sinai-Derrida model. With similar reasoning we assume $c \ll T$ for the coherent hopping. The vertical axis of the diagram is the quantum parameter η that reflects the ratio between ν and T_{bath}. It is the same dimensionless "friction" parameter that appears is the analysis of the spin-boson Hamiltonian. The validity of the Ohmic master equation requires $\eta \ll 1$. In the regime $\eta > 1$ the model is not valid because non-Markovian memory effects cannot be neglected.

The first inequality in Eq. (23) means that we regard the coherent effects as a perturbation with respect to the dominant stochastic dynamics. This stands in opposition to the common quantum-dissipation studies, where the bath is regraded as a disturbance that slightly spoils or modifies coherent evolution. In the regime diagram the border between the two regimes is represented by the diagonal line $\eta = \sigma_f$.

In our mathematical analysis T_{bath} merely determines the ratio $\sigma_{\mathcal{E}}/\sigma_f$ and should be kept larger than $\nu \equiv 1$ in accordance with Eq. (23). To avoid misunderstanding, we emphasize that from an experimental perspective the physical temperature affects the parameters ν and σ_f. Therefore, setting $\eta = \infty$ in the sense of Eq. (2), while *fixing* the transition rates, does not really corresponds to zero temperature and furthermore contradicts our assumption Eq. (23).

V. THE NONDISORDERED RING

For nondisordered ring with $c = 0$ the Lindblad equation becomes identical with the Pauli master equation, namely the diagonal elements p_x of the probability matrix $\rho_{x', x''}$ satisfy the rate equation Eq. (4), while each diagonal term satisfies the equation

$$\frac{d}{dt}\rho_r = [-\gamma - (w^+ + w^-) + i\mathcal{E}r]\rho_r \tag{24}$$

with $r = (x' - x'') = \pm 1, \pm 2, \cdots$. We conclude that the eigenvalues $\{-\lambda_{q,r}\}$ of $\mathcal{L}$ are

$$\lambda_{q,r=0} = (w^+ + w^-)[1 - \cos(q)] - i(w^+ - w^-)\sin(q), \tag{25}$$

$$\lambda_{q,r\neq0} = \gamma + (w^+ + w^-) - i\mathcal{E}r, \tag{26}$$

where the wave number is $q = (2\pi/N) \times$ integer. Accordingly, we distinguish between *relaxation-modes* that have eigenvalues $\lambda_{q,0}$ and *decoherence-modes* that have eigenvalues $\lambda_{q,r\neq0}$. This distinction is blurred for $c \neq 0$ due to mixing of the r branches, but nevertheless it can be maintained for small c (see below), even in the presence of disorder (see next section).

We can extract the drift velocity v and the diffusion coefficient D from the expansion

$$\lambda_{q,0} \approx ivq + Dq^2 + \mathcal{O}(q^3). \tag{27}$$

For nondisordered $c = 0$ ring, Eq. (26) implies, as expected, the trivial results $v = (w^+ - w^-)$ and $D = (w^+ + w^-)/2$.

Next we explore how the spectrum is modified for $c \neq 0$. An example for the outcome of numerical diagonalization is provided in Fig. 3. The dependence on c is illustrated. Below we explain the observed dependence analytically.

The hopping couples the diagonal and the off diagonal terms of $\rho_{x', x''}$. It is convenient to define a position coordinate $x = (x' + x'')/2$ and a transverse coordinate $r = (x' - x'')$. Then we can define an operator $\boldsymbol{r} = \sum_r |r\rangle r\langle r|$, a displacement operator $\mathcal{D}_\perp$ is the transverse r coordinate, and a displacement operator e^{-iq} in the x coordinate. The total Lindbladian can be regarded as a non-Hermitian Hamiltonian that generates dynamics on an (x, r) lattice, see Fig. 4. It can be expressed as follows:

$$\mathcal{L} = -\gamma_0 + (\gamma_0 - \mathcal{W}) \otimes |0\rangle\langle0|$$
$$- i\mathcal{E}\boldsymbol{r} - c\sin(\boldsymbol{q}/2)[\mathcal{D}_\perp - \mathcal{D}_\perp^\dagger], \tag{28}$$

where $\gamma_0 \equiv \gamma + w^+ + w^-$. More generally, we define $\gamma_q \equiv \gamma + w^+ e^{-iq} + w^- e^{iq}$. In the absence of disorder the lattice has Bloch translation symmetry in x, and therefore q is a good quantum number. The q block of the Lindbladian is

$$\mathcal{L}^{(q)} = -\gamma_0 + \gamma_q|0\rangle\langle0| - i\mathcal{E}\boldsymbol{r} - c\sin(q/2)[\mathcal{D}_\perp - \mathcal{D}_\perp^\dagger]. \tag{29}$$

For clarity, and for further analysis, we write a truncated matrix version of $\mathcal{L}^{(q)}$, where we keep only $r = -1, 0, 1$. Namely

$$\mathcal{L}^{(q)} = \begin{bmatrix} -\gamma_0 + i\mathcal{E} & c\sin(q/2) & 0 \\ -c\sin(q/2) & -\gamma_0 + \gamma_q & c\sin(q/2) \\ 0 & -c\sin(q/2) & -\gamma_0 - i\mathcal{E} \end{bmatrix}. \tag{30}$$

In section 4 of the supplementary material of Ref. [15] (see also Ref. [16]), the following result has been derived:

$$\lambda_{q,0} = \gamma_0 - \sqrt{\gamma_q^2 - 4c^2\sin^2(q/2)}. \tag{31}$$

This result allows finite f_{bias} but neglects $\mathcal{E}_{\text{bias}}$.

The eigenvalues of $\mathcal{L}^{(q)}$ are labeled $\lambda_{q,s}$, with band index $s = 0, \pm1, \pm2, \cdots$ that distinguishes the $s = 0$ relaxation modes from the $s \neq 0$ decoherence modes. The former correspond to the eigenvalues of $\mathcal{W}$. The distinction between *relaxation modes* and *decoherence modes* remains meaningful for small c, as long as the bands remain separated. In Fig. 3 only the eigenvalues of the relaxation modes are displayed. As c becomes larger, the Im(λ) of the relaxation modes increases monotonically. The numerical diagonalization agrees with Eq. (31) and approximately with diagonalization of the truncated version Eq. (30).

VI. THE EFFECT OF DISORDER

The matrix $\mathcal{W}$ is real. Therefore its characteristic polynomial is real, and accordingly its eigenvalues λ_q are either real or complex-conjugate pairs. Note that in the absence of disorder q can be interpreted as quasimomentum, while in the presence of disorder q becomes a dummy index. The delocalization of eigenmodes, as f_{bias} in increased, is indicated
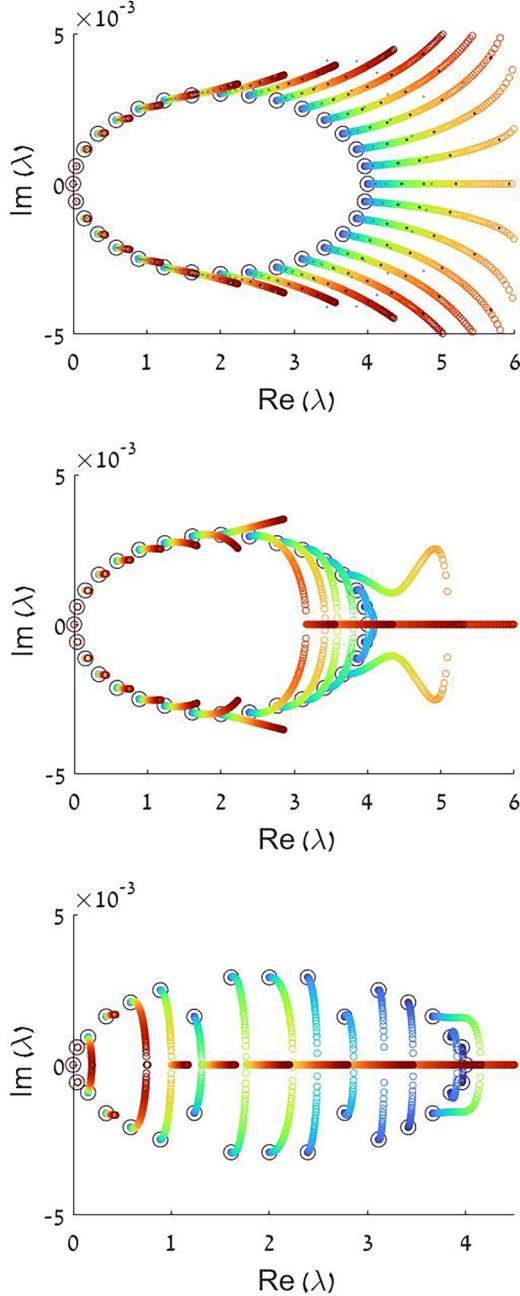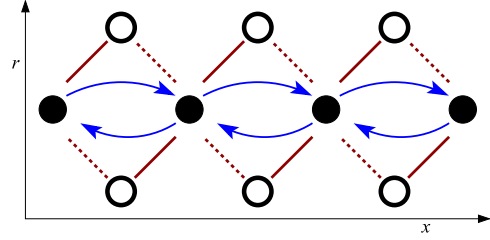
FIG. 4. Diagrammatic representation of the lattice. The axes are x and r. Only the $r = -1, 0, 1$ elements are displayed. Bath-induced $w^{\pm}$ transitions are colored in blue: They connect only $r = 0$ elements. Coherent $\pm i(c/2)$ transverse transitions are indicated by solid and dashed red lines.

with large Re(λ), become complex. Figure 2 illustrates this delocalization scenario, showing how the number of complex eigenvalues depends on f for a range of σ_f values.

A similar scenario is expected for the Lindbladian $\mathcal{L}$. The hermiticiy of ρ implies that the supermatrix $\mathcal{L}_{n',m'|n'',m''}$ is complex conjugated if we perform the reflection $\mathcal{R} : (n, m) \mapsto (m, n)$. So we have the relation $\mathcal{R}\mathcal{L}\mathcal{R} = \mathcal{L}^*$. This implies that the characteristic polynomial of $\mathcal{L}$ is real, as in the case of $\mathcal{W}$.

A. The relaxation spectrum

The relaxation spectrum of a disordered ring for $c \neq 0$ is illustrated in Fig. 3. Note that we use the same ring as in Fig. 2, with the same disorder realization. Different values of σ_f are achieved by uniform "stretching" of the field values, without affecting the relative magnitudes. The major counterintuitive observation is as follows: The introduction of coherent hopping is qualitatively similar to *stronger* disorder. This is reflected by the migration of eigenvalues towards the real axis. The effect is pronounced for eigenvalues with larger Re(λ), namely eigenvalues with larger Re(λ) are more sensitive to c.

B. Identification of the relaxation spectrum

It is very easy to identify the perturbed $\lambda_{q,0}$ branch of the spectrum if γ is large, because large γ shifts all the $\lambda_{q,s \neq 0}$ eigenvalues to Re(λ) $\sim 2\nu + \gamma$. But if, say, $\gamma = 0$, we can still try to identify this branch by calculating the diagonal norm Q of each eigenmode. A given eigenmode ρ of the supermatrix $\mathcal{L}$ can be regarded as a supervector, with the ad hoc normalization $\sum_{x,x'} |\rho_{x,x'}|^2 = 1$. What we call diagonal norm is the partial sum $Q = \text{trace}(\rho)$. In Fig. 5 we demonstrate that in the range of interest this procedure allows to isolate the $\lambda_{q,0}$ branch, even if $\gamma = 0$. The points are color coded by the inverse participation ratio, namely IPR = $\sum_{x,x'} |\rho_{x,x'}|^4$. Large IPR for a relaxation-mode indicates localization (only small number of sites participate).

VII. EFFECTIVE DISORDER

In order to understand analytically the observed dependence of the spectrum on c, we write the equation $\mathcal{L}\rho = -\lambda\rho$ for the elements (x, $r = -1, 0, 1$) of ρ, based on the diagram of Fig. 4. Then we eliminate the $r = \pm 1$ elements, expressing

FIG. 3. The Lindblad spectrum. Spectra of the Lindbladian for the same ring as in Fig. 2, with $\sigma_\nu = 0$, while the dispersion of the stochastic field is $\sigma_f = 0$ (upper panel), $\sigma_f = 0.005$ (middle panel), and $\sigma_f = 0.02$ (lower panel). The color code indicates the value of c. It goes from blue ($c = 0$) to red ($c = 2$). The bias is $f = 0.003$. The temperature is $T_{\text{bath}} = 200$, and the on-site decoherence rate is $\gamma = 5$. The black circles indicate the spectrum of $\mathcal{W}$. In the upper panel the black dots are from Eq. (31), while the gray dots are from the perturbative approximation based on Eq. (30). The eigenvalues that correspond to the decoherence modes Eq. (26) are outside of the axis borders.

by the formation of complex-conjugate pairs. The eigenvalues at the vicinity of $\lambda \sim 0$ are the first to get delocalized, indicating a crossover from overdamped to underdamped relaxation [11,12]. For very large f_{bias} most of the eigenvalues, also those
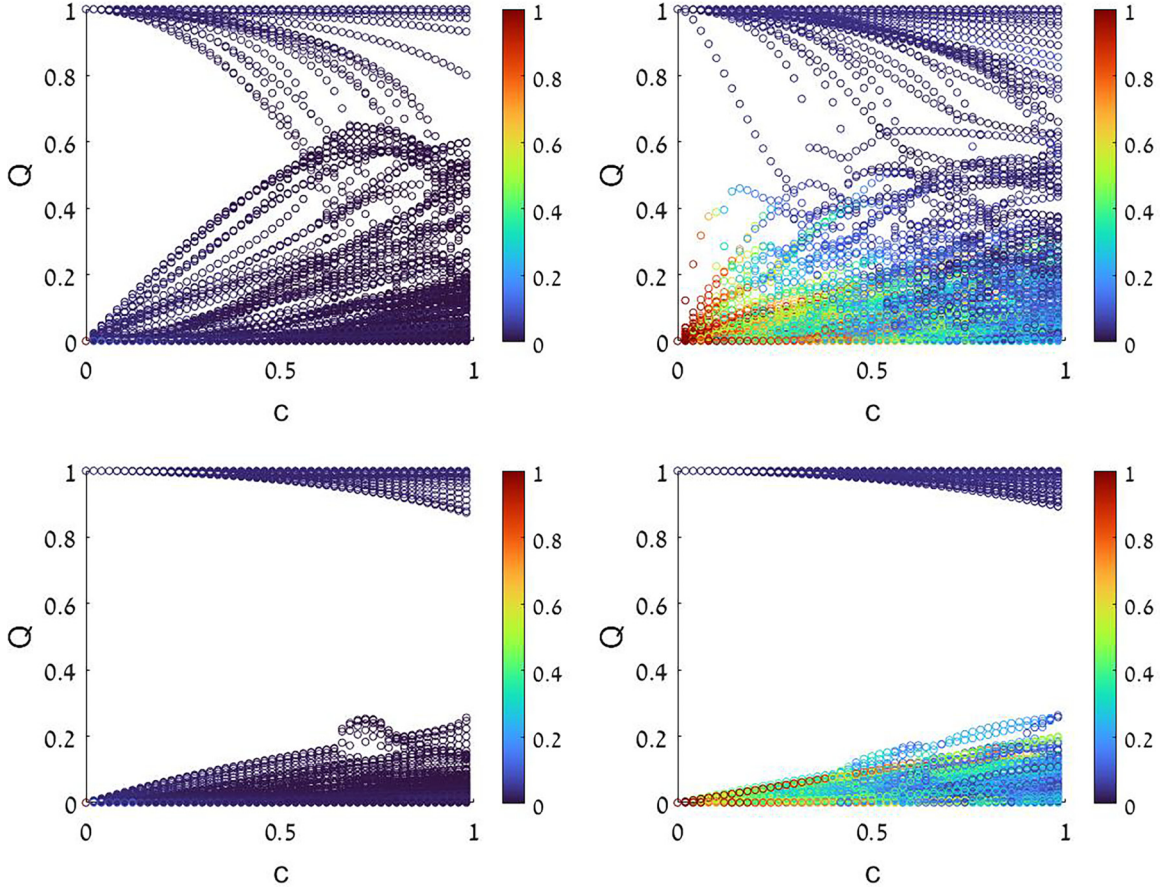
FIG. 5. The diagonal norm versus c. We consider the same ring as in Fig. 2 with $\gamma = 0$ (upper panels) and $\gamma = 5$ (lower panels). For a given value of c we calculate the diagonal norm Q and the IPR (color coded) for each eigenmode. The measure Q allows to distinguish the $s = 0$ branch from the other branches. As c is increased the branches get mixed. The left panels are for zero disorder, while the right panels are for $\sigma_f = 0.02$.

them in terms of the $r = 0$ elements. Substitution into the equation for the $r = 0$ elements, we conclude that the effective transition rates are modified as follows:

$$\nu_x^{\text{effective}} = \nu_x + \frac{c^2}{2} \frac{(\lambda - \gamma_x)}{(\lambda - \gamma_x)^2 + \mathcal{E}_x^2}. \qquad (32)$$

This formula allows us to estimate how different eigenvalues along the $\lambda_{q,0}$ branch are affected by the disorder. Let us start our reasoning with the assumption that the bias is small or even zero. Accordingly, the relaxation spectrum is real. Equation (32) implies that that the introduction of c is equivalent to an effective resistor-network disorder with dispersion σ_ν that is proportional to $\sigma_{\mathcal{E}}$. For the purpose of rough estimate one can substituted $(\lambda - \gamma_x) \mapsto \nu$. Then it follows that

$$\sigma_\nu \sim \frac{c^2}{\nu^3} T_{\text{bath}}^2 \, \sigma_f^2, \qquad (33)$$

where we used $\mathcal{E}_{\text{bias}} \ll \sigma_{\mathcal{E}} \ll \nu$ and the relation Eq. (1).

A. Localization

Due to σ_f and σ_ν the eigenmodes of the chain are localized. As the bias is increased gradually from zero, one expects a delocalization transition. We shall discuss this tran-

sition analytically in the next section. We can also go in the other direction. Namely, we fix a relatively large bias such that the relaxation eigenmodes are delocalized, with complex eigenvalues λ_q. Then we increase the disorder and/or c gradually to see how the spectrum is affected. We discuss this scenario further below.

In the absence of disorder the introduction of c leads to monotonic increase of $\text{Im}(\lambda_q)$, as implied by Eq. (31). This effect is not uniform: The eigenvalues in the vicinity of $\lambda \sim 0$ are hardly affected.

In the presence of weak disorder the dependence of $\text{Im}(\lambda_q)$ on c becomes nonmonotonic, see Fig. 3, reflecting a crossover from a non-disordered-like dependence that is implied by Eq. (31) to the disordered-case dependence that is implied by Eq. (32). Namely, the implication of the effective disorder is to "push" towards localization, and hence $\text{Im}(\lambda_q)$ is decreased.

If the effective-disorder is strong enough, the eigenvalues become real, indicating localization. Also here the effect is not uniform: The eigenvalues in the vicinity of $\lambda \sim 0$ are hardly affected. We explain this observation in the next section.

B. Global localization

The global localization of the relaxation modes as a function of σ_f for different values of f has been illustrated in lower
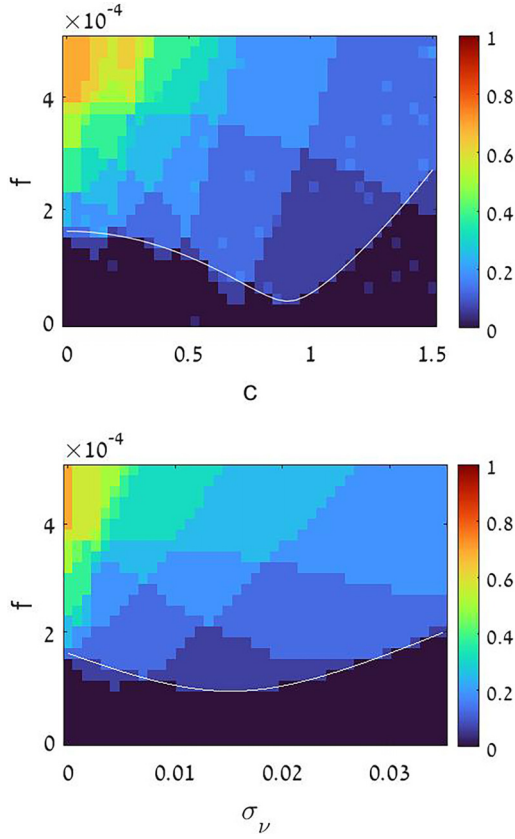
FIG. 6. Enhanced effective disorder. We consider the sample of Fig. 2 with $\sigma_f = 0.01$. Upper panel: The relaxation spectrum is obtained from the diagonalization of the Lindbladian $\mathcal{L}$, with $\sigma_v = 0$. The bath temperature is $T_{\text{bath}} = 800$, and the on-site decoherence rate is $\gamma = 10$. The color-code indicates the results for N_{cmplx}/N, and the axes are c and f. Lower panel: The results are based on diagonalization of the associated $\mathcal{W}$, and the axes are σ_v and f. Comparing with the upper panel one observes qualitative correspondence. Note that different samples exhibit different dependence on the strength of the effective disorder. Monotonic dependence is found only after statistical averaging.

panel of Fig. 2. In the upper panel of Fig. 6 we demonstration how this localization is affected by c. We also demonstrate there (in the lower panel) that the effect of c can be mimicked by introducing into $\mathcal{W}$ an effective resistor-network-disorder. However, this should not be overstated. It should be clear that the details of the crossover from nondisordered ring cannot be captured by a purely stochastic model, because the former features a nonmonotonic dependence of the eigenvalues on c.

The delocalization threshold f_c is related to the eigenvalues that reside at the vicinity of $\lambda = 0$, while the global count N_{cmplx} of complex eigenvalues probes the delocalization globally. For the particular disorder-realization of Fig. 6 the dependence on the strength of the disorder is rather monotonic for N_{cmplx} but not monotonic for f_c. For other disorder-realizations the dependence of f_c on the strength of disorder is different. It is only after averaging, over many realizations, that we get a monotonic dependence. Furthermore, we clarify below that the dependence of f_c on c is diminished for large rings.
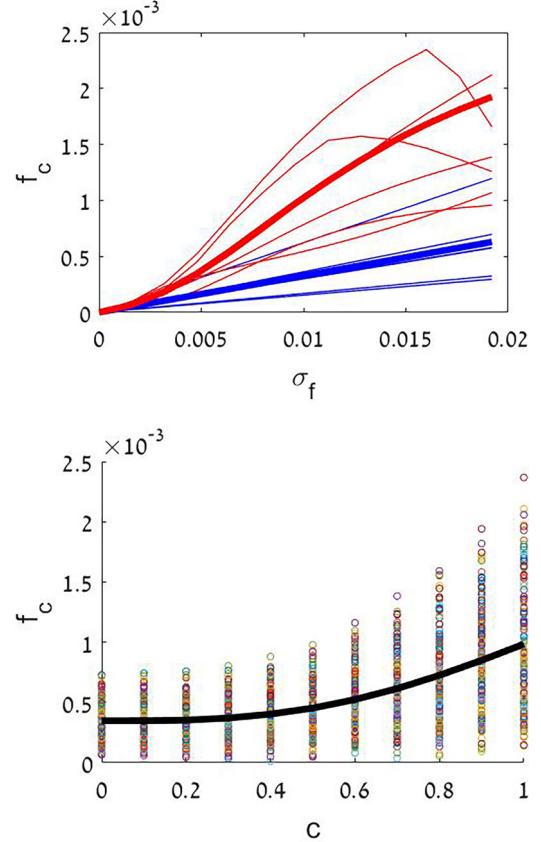

FIG. 7. Delocalization threshold versus model parameters. The upper panel, f_c versus σ_f, is obtained by averaging over 150 realizations of disorder for $c = 0$ (thick blue line) and $c = 1$ (thick red line). Thin lines illustrate the nonaveraged results for six randomly selected realizations. The lower panel, f_c versus c, is for realizations with $\sigma_f = 0.01$. The symbols illustrate the values before averaging. The bath temperature is $T_{\text{bath}} = 200$, and the on-site decoherence is $\gamma = 0$.

The average dependence of f_c on σ_f and c is illustrated in Fig. 7. We also provide the results for a few randomly selected realizations (thin lines) to illustrate the fluctuations. Figure 8 displays the full histograms for the 150 disorder realizations. We see that for larger rings the effect of c on f_c is diminished. This observation will be explained in the next section.

On the other hand, the *global* effect of c is not diminished for large N. For that we have to look globally on the spectrum and not just at the vicinity of $\lambda \sim 0$. To quantify this statement we find for a given f_{bias} the critical value σ_{critical} of σ_f above which real eigenvalues appear, indicating localization of some "remote" eigenmodes. One observes in the right histogram of Fig. 8 that the effect of c does not diminish for longer samples.

VIII. THE DELOCALIZATION THRESHOLD

The localization of the relaxation modes is due to the σ_f disorder and also influenced by the σ_v disorder. The latter is enhanced once coherent hopping is introduced, as implied by Eq. (32).

For the purpose of analysis one introduces an Hermitian matrix $\mathcal{H}_W$ that is associated with $\mathcal{W}$. Using the same
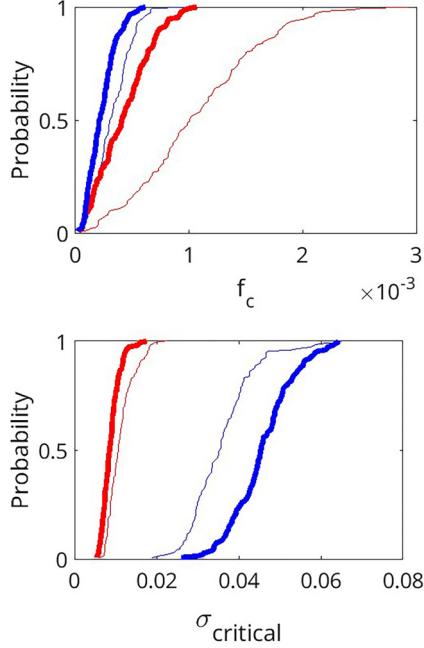
FIG. 8. Delocalization threshold statistics. Cumulative histograms for f_c given $\sigma_f = 0.01$ and for σ_{critical} given $f_{\text{bias}} = 0.003$. The thick lines are for $N = 64$, while the thin lines are for $N = 32$. The blue and the red lines are for $c = 0$ and for $c = 1$, respectively. The histograms are based on 150 realizations of the disorder.

notations as in Eq. (9) the associated matrix is

$$\mathcal{H}_W = \text{diagonal}\left\{(v_x + v_{x-1}) + \frac{v}{2}(f_x - f_{x-1}) + \frac{v}{4}f^2\right\}$$
$$- \text{off-diagonal}\{v_x\}. \quad (34)$$

The following relation exists [5–7,11]:

$$\det(\lambda + \mathcal{W}) = \det(\lambda - \mathcal{H}_W)$$
$$- 2\left[\cosh\left(\frac{Nf}{2}\right) - 1\right]\prod_x(-v_x). \quad (35)$$

Consequently, one can write the characteristic equation for the eigenvalues as $F(\lambda) = F(0)$, where

$$F(\lambda) = \frac{1}{N}\sum_{k=0}^{N}\ln\left|\frac{\lambda - \epsilon_k}{v_{\text{avg}}}\right|. \quad (36)$$

Here ϵ_k are the eigenvalues of $\mathcal{H}_W$, and v_{avg} is the geometric average over the v_x. The right-hand side of the equation $F(\lambda) = F(0)$ is implied by the simple observation that $\lambda = 0$ should be a trivial root of the characteristic equation.

The envelope $\kappa(\lambda)$ of the function $F(\lambda)$ is identified as the Thouless formula for the inverse localization length of eigenstates that are associated with ϵ_k. Consequently, the condition for getting complex eigenvalues from the equation $F(\lambda) = F(0)$ is $\kappa(\lambda) < F(0)$. Below we explain the derivation of the following expression:

$$\kappa(\lambda) \approx \alpha_0 f_c - \alpha_c \frac{(f - f_c)}{f_c}\sqrt{\frac{\lambda}{v}} + \frac{\sigma_v^2}{8v^3}\lambda, \quad (37)$$

where f_c, which is given by Eq. (10), is independent of σ_v, while α_0 and α_c are numerical constants. From this expression it follows that for $f > f_c$ complex roots appear at the vicinity of $\lambda \sim 0$. This threshold is not affected by σ_v and therefore also not affected by c. However, the resistor network disorder enhances the localization for larger λ and therefore affects the *global* delocalization of the eigenmodes.

The derivation of Eq. (37) requires the integration of several ingredients that have been worked out in past studies. We provide here an outline how to obtain this formula. The basic observation of Derrida and followers is that $\mathcal{W}$ generates anomalous spreading $|x| \sim t^\mu$ that is characterized by an exponent μ. This exponent is determined through the equation $\langle e^{-\mu f_x}\rangle = 1$. It is important to realize that μ is rigorously independent of the resistor-network disorder. For Gaussian distribution one obtains the relation $\mu = (2/\sigma_f^2)f$.

It is implied by the anomalous spreading that the density of the eigenvalues ϵ_k at the bottom of the "energy" band is $\epsilon^{\mu-1}$. This can be used in the Thouless relation to derive the result $F'(\lambda) \approx (\lambda^{\mu-1}/v^\mu)\pi\mu\cot(\pi\mu)$. See Ref. [11] for details. It follows that complex eigenvalues appear near the origin for $\mu > \mu_c$ where $\mu_c = (1/2)$. The second term in Eq. (37) is obtained after linearization of $F'(\lambda)$ around this critical value.

The first and the third terms in Eq. (37) correspond to the correlated Anderson diagonal-disorder and to the Debye-resistor-network off-diagonal disorder that we have in Eq. (34). Section VII of Ref. [14], including Appendix C there, provide a fair presentation for these two types of disorder. The estimation of the inverse localization length is performed using the Born approximation (Fermi golden rule). The Debye disorder provides a term that is proportional to $[\text{Var}(v_x)]\lambda$. This contribution vanishes at the bottom of the energy band as expected. The Anderson disorder provides a term that is proportional to $[\text{Var}(\text{diagaonl})]/\lambda$, where $\text{Var}(\text{diagaonl})$ is the effective variance of the diagonal terms. Here one should notice that $f_x - f_{x-1}$ in Eq. (34) features telescopic correlations, and hence $\text{Var}(\text{diagaonl}) \propto [\text{Var}(f)]\lambda$ is proportional to λ. Consequently the Anderson term in Eq. (37) is independent of λ.

IX. SUMMARY

Quantum Brownian motion is a well-studied theme (see Refs. [17–20] and references within). In the condensed-matter literature it is common to refer to the Caldeira-Leggett model [21,22], where the particle is linearly coupled to the modes of an Ohmic environment. The strongly related problem of motion in a tight binding lattice [23–26] can be regarded as a natural extension of the celebrated spin-boson model. The cited works assume that the fluctuations are uniform in space. Some other works consider the dynamics of a particle that interacts with local baths. In such models the fluctuations acquire finite correlations in space [16,27–37]. More recently, the basic question of transport in a tight-binding lattice has resurfaced in the context of excitation transport in photosynthetic light-harvesting complexes [38–47].

Considering the possibility that each site and each bond experiences a different local bath, it is puzzling that all of the above cited works have somehow avoided the confrontation of themes that are familiar from the study of stochastic

motion in random environment. Specifically we refer here to the extensive work by Sinai, Derrida, and followers [1–4], and the studies of stochastic relaxation [11,12] which is related to the works of Hatano, Nelson, and followers [5–10].

In order to bridge this gap, we have introduced in an earlier paper [15] a quantized version of the Sinai-Derrida model. In the present work we have considered a simplified version that captures the essential physics. Without coherent hopping ($c = 0$) it reduces to the Pauli master equation and hence becomes identical to the standard Sinai-Derrida model. The model features two dimensionless parameters that control its regime diagram Fig. 1. The smallness of the quantum parameter $\eta \ll 1$ implies that memory effects can be neglected, and hence we can use a Lindblad version of the Ohmic master equation. The smallness of the classical parameter $\sigma_f \ll 1$ reflects the standard assumption of weak stochastic disorder, as in the original model of Sinai.

The Hatano-Nelson delocalization transition is related to the Sinai-Derrida sliding transition. We find that adding coherent transitions "in parallel" to the stochastic transitions leads to some counterintuitive effects. In order to illustrate these effects we have inspected mainly two measures: (a) the overall number of complex (underdamped) relaxation modes and (b) the threshold f_c for underdamped relaxation. The latter measure focuses on the eigenvalues at the vicinity of $\lambda \sim 0$. The main observations are as follows: (1) The relaxation modes are strongly affected by coherent hopping, (2) the dependence of Imλ on c becomes nonmonotonic, (3) on-site decoherence affects the sensitivity to the c dependence, (4) some features of the localization transition can be mimicked by introducing an effective random-resistor network disorder in the stochastic description, (5) the dependence of the delocalization threshold on c is very weak for large rings, and (6) the delocalization threshold for small quantum rings exhibits strong fluctuations.

Our observations regarding delocalization concern the regime $c \ll \nu$, within the region where the coherent hopping can be regarded as a perturbation. This means that the relaxation modes are distinct and well separated form the decoherence modes. This allows a meaningful comparison with the stochastic model.

APPENDIX: THE LINDBLAD MASTER EQUATION

A master equation for the time evolution of the system probability matrix ρ is of Lindblad form if it can be written as

$$\frac{d\rho}{dt} = -i[\boldsymbol{H}, \rho] + \sum_x \nu_x \left[\boldsymbol{L}_x \rho \boldsymbol{L}_x^\dagger - \frac{1}{2}\{\boldsymbol{L}_x^\dagger \boldsymbol{L}_x, \rho\} \right]$$

$$= -i[\boldsymbol{H}, \rho] - \frac{1}{2}(\boldsymbol{\Gamma}\rho + \rho\boldsymbol{\Gamma}) + \sum_x \nu_x \boldsymbol{L}_x \rho \boldsymbol{L}_x^\dagger. \quad \text{(A1)}$$

Here we consider interaction with *local* baths that are coupled to the sites or to the bonds, hence the index x indicates posi-

tion. We have defined

$$\boldsymbol{\Gamma} = \sum_x \nu_x \boldsymbol{L}_x^\dagger \boldsymbol{L}_x. \quad \text{(A2)}$$

A Lindblad generator due to coupling to an an Ohmic bath can be written as

$$\boldsymbol{L} = \boldsymbol{W} + i\frac{\eta}{2\nu}\boldsymbol{V}, \quad \text{(A3)}$$

where it has been assumed that the coupling to bath coordinate is $-\boldsymbol{W}F_{\text{bath}}$. The fluctuations of F are charaterized by intensity ν ("noise") and asymmetry η ("friction"), while $\boldsymbol{V} \equiv i[\boldsymbol{H}, \boldsymbol{W}]$. Note that in the Fokker Planck equation $\boldsymbol{W}$ is the position coordinate, and $\boldsymbol{V}$ is the velocity operator.

1. Bond dissipators

The interaction with a bath-source that induces noncoherent transitions at a given bond is obtained by the replacement $(c/2) \mapsto (c/2) + f(t)$ in the respective term of the Hamiltonian. Accordingly,

$$\boldsymbol{W}_x^{(B)} = (\boldsymbol{D}_x + \boldsymbol{D}_x^\dagger), \quad \text{(A4)}$$

$$\boldsymbol{V}_x^{(B)} = i[\boldsymbol{H}, \boldsymbol{W}_x]$$

$$= i\mathcal{E}_x(\boldsymbol{D}_x^\dagger - \boldsymbol{D}_x) - i\frac{c}{2}[(\boldsymbol{D}_{x+1}\boldsymbol{D}_x - \boldsymbol{D}_x\boldsymbol{D}_{x-1}) - \text{H.c.}]. \quad \text{(A5)}$$

Neglecting the double hopping term the Lindblad generators Eq. (A3) are

$$\boldsymbol{L}_x^{(B)} = \left(1 + \frac{f_x}{4}\right)\boldsymbol{D}_x + \left(1 - \frac{f_x}{4}\right)\boldsymbol{D}_x^\dagger, \quad \text{(A6)}$$

where

$$f_x = \frac{2\eta_x \mathcal{E}_x}{\nu_x} \equiv \frac{\mathcal{E}_x}{T_x}. \quad \text{(A7)}$$

We identify the rates of transitions

$$w_x^\pm = \left(1 \pm \frac{f_x}{2}\right)\nu_x = \nu_x \pm \eta_x \mathcal{E}_x. \quad \text{(A8)}$$

Plugging Eq. (A6) into Eq. (A2), using Eq. (A8) and the identity $\boldsymbol{D}_x^\dagger \boldsymbol{D}_x = \boldsymbol{Q}_x$, we get

$$\boldsymbol{\Gamma}^{(B)} = \sum_x (w_x^+ + w_{x-1}^-)\boldsymbol{Q}_x = (w^+ + w^-), \quad \text{(A9)}$$

where the last expression applies if the rates do not depend on x (no disorder). Then from Eq. (A1) we get

$$\mathcal{L}^{(B)}\rho = -(w^+ + w^-)\rho + \sum_x [w^+ \boldsymbol{D}_x^\dagger \rho \boldsymbol{D}_x + w^- \boldsymbol{D}_x \rho \boldsymbol{D}_x^\dagger$$

$$+ \nu \boldsymbol{D}_x \rho \boldsymbol{D}_x + \nu \boldsymbol{D}_x^\dagger \rho \boldsymbol{D}_x^\dagger]. \quad \text{(A10)}$$

More generally, with disorder, we get $\mathcal{L}^{(B)}$ of Eq. (11), that has been simplified by dropping the last two terms. The omitted terms merely modify the lowest decoherence modes as discussed in Ref. [15].

2. Site dissipators

Optionally we can add terms that reflect fluctuations of the field. At a given site it is obtained by the replacement

$U(\boldsymbol{x}) \mapsto U(\boldsymbol{x}) + \tilde{f}(t)$, where $\tilde{f}(t)$ represents fluctuations of intensity γ. The implied coupling operators are

$$\boldsymbol{W}_x^{(S)} = \boldsymbol{Q}_x, \tag{A11}$$

$$\boldsymbol{V}_x^{(S)} = i[\boldsymbol{H}, \boldsymbol{W}_x^{(S)}] = i(c/2)[(\boldsymbol{D}_{x-1}^\dagger - \boldsymbol{D}_{x-1}) - (\boldsymbol{D}_x^\dagger - \boldsymbol{D}_x)]. \tag{A12}$$

Neglecting the hopping effect the Lindblad generator is $\boldsymbol{L}_x^{(S)} = \boldsymbol{Q}_x$. To avoid confusion we use γ_x instead of ν_x for the intensity of the bath-induced noise. Plugging into Eq. (A2) we get

$$\boldsymbol{\Gamma}^{(S)} = \sum_x \gamma_x \boldsymbol{Q}_x = \gamma, \tag{A13}$$

where the last expression applies if the γ_x do not depend on x.

[1] Y. G. Sinai, The limiting behavior of a one-dimensional random walk in a random medium, Theory Probab. Appl. **27**, 25 (1982).

[2] B. Derrida, Velocity and diffusion constant of a periodic one-dimensional hopping model, J. Stat. Phys. **31**, 433 (1983).

[3] J. P. Bouchaud, A. Comtet, A. Georges, and P. Le-Doussal, Classical diffusion of a particle in a one-dimensional random force field, Ann. Phys. **201**, 285 (1990).

[4] J. P. Bouchaud and A. Georges, Anomalous diffusion in disordered media: Statistical mechanisms, models and physical applications, Phys. Rep. **195**, 127 (1990).

[5] N. Hatano and D. R. Nelson, Localization transitions in non-Hermitian quantum mechanics, Phys. Rev. Lett. **77**, 570 (1996).

[6] N. Hatano and D. R. Nelson, Vortex pinning and non-Hermitian quantum mechanics, Phys. Rev. B **56**, 8651 (1997).

[7] N. M. Shnerb and D. R. Nelson, Winding numbers, complex currents, and non-Hermitian localization, Phys. Rev. Lett. **80**, 5172 (1998).

[8] J. Feinberg and A. Zee, Non-Hermitian localization and delocalization, Phys. Rev. E **59**, 6433 (1999).

[9] Y. Kafri, D. K. Lubensky, and D. R. Nelson, Dynamics of molecular motors and polymer translocation with sequence heterogeneity, Biophys. J. **86**, 3373 (2004).

[10] Y. Kafri, D. K. Lubensky, and D. R. Nelson, Dynamics of molecular motors with finite processivity on heterogeneous tracks, Phys. Rev. E **71**, 041906 (2005).

[11] D. Hurowitz and D. Cohen, Percolation, sliding, localization and relaxation in topologically closed circuits, Sci. Rep. **6**, 22735 (2016).

[12] D. Hurowitz and D. Cohen, Relaxation rate of a stochastic spreading process in a closed ring, Phys. Rev. E **93**, 062143 (2016).

[13] D. Shapira and D. Cohen, Emergence of Sinai Physics in the stochastic motion of passive and active particles, New J. Phys. **24**, 063026 (2022).

[14] D. Boriskovsky and D. Cohen, Negative mobility, sliding and delocalization for stochastic networks, Phys. Rev. E **101**, 062129 (2020).

[15] D. Shapira and D. Cohen, Quantum stochastic transport along chains, Sci. Rep. **10**, 10353 (2020).

[16] M. Esposito and P. Gaspard, Exactly solvable model of quantum diffusion, J. Stat. Phys. **121**, 463 (2005).

[17] J. Schwinger, Brownian motion of a quantum oscillator, J. Math. Phys. **2**, 407 (1961).

[18] V. Hakim and V. Ambegaokar, Quantum theory of a free particle interacting with a linearly dissipative environment, Phys. Rev. A **32**, 423 (1985).

[19] H. Grabert, P. Schramm, and G. L. Ingold, Quantum Brownian motion: The functional integral approach, Phys. Rep. **168**, 115 (1988).

[20] P. Hänggi and G. L. Ingold, Fundamental aspects of quantum Brownian motion, Chaos: An Interdisciplinary J. Nonlin. Sci. **15**, 026105 (2005).

[21] A. O. Caldeira and A. J. Leggett, Path integral approach to quantum Brownian motion, Physica A **121**, 587 (1983).

[22] A. O. Caldeira and A. J. Leggett, Quantum tunnelling in a dissipative system, Ann. Phys. **149**, 374 (1983).

[23] U. Weiss and H. Grabert, Quantum diffusion of a particle in a periodic potential with ohmic dissipation, Phys. Lett. A **108**, 63 (1985).

[24] C. Aslangul, N. Pottier, and D. Saint-James, Quantum ohmic dissipation: Cross-over between quantum tunnelling and thermally resisted motion in a biased tight-binding lattice, J. Phys. **47**, 1671 (1986).

[25] C. Aslangul, N. Pottier, and D. Saint-James, Quantum Brownian motion in a periodic potential: A pedestrian approach, J. Phys. France **48**, 1093 (1987).

[26] U. Weiss, M. Sassetti, T. Negele, and M. Wollensak, Dissipative quantum dynamics in a multiwell system, Z. Phys. B **84**, 471 (1991).

[27] D. Shapira and D. Cohen, Breakdown of quantum-to-classical correspondence for diffusion in high temperature thermal environment, Phys. Rev. Res. **3**, 013141 (2021).

[28] D. Cohen, Unified model for the study of diffusion localization and dissipation, Phys. Rev. E **55**, 1422 (1997).

[29] A. Madhukar and W. Post, Exact solution for the diffusion of a particle in a medium with site diagonal and off-diagonal dynamic disorder, Phys. Rev. Lett. **39**, 1424 (1977).

[30] N. Kumar and A. M. Jayannavar, Quantum diffusion in thin disordered wires, Phys. Rev. B **32**, 3345 (1985).

[31] D. Roy, Crossover from ballistic to diffusive thermal transport in quantum Langevin dynamics study of a harmonic chain connected to self-consistent reservoirs, Phys. Rev. E **77**, 062102 (2008).

[32] A. Amir, Y. Lahini, and H. B. Perets, Classical diffusion of a quantum particle in a noisy environment, Phys. Rev. E **79**, 050105(R) (2009).

[33] S. Lloyd, M. Mohseni, A. Shabani, and H. Rabitz, Thequantum Goldilocks effect: On the convergence of timescales in quantum transport, arXiv:1111.4982.

[34] J. M. Moix, M. Khasin, and J. Cao, Coherent quantum transport in disordered systems: I. The influence of dephasing on the transport properties and absorption spectra on one-dimensional systems, New J. Phys. **15**, 085010 (2013).

[35] J. Wu, R. J. Silbey, and J. Cao, Generic mechanism of optimal energy transfer efficiency: A scaling theory of the mean first-passage time in exciton systems, Phys. Rev. Lett. **110**, 200402 (2013).

[36] Y. Zhang, G. L. Celardo, F. Borgonovi, and L. Kaplan, Opening-assisted coherent transport in the semiclassical regime, Phys. Rev. E **95**, 022122 (2017).

[37] Y. Zhang, G. L. Celardo, F. Borgonovi, and L. Kaplan, Optimal dephasing for ballistic energy transfer in disordered linear chains, Phys. Rev. E **96**, 052103 (2017).

[38] H. van Amerongen, R. van Grondelle, and L. Valkunas, *Photosynthetic Excitons* (World Scientific, Singapore, 2000).

[39] T. Ritz, A. Damjanović, and K. Schulten, The quantum physics of photosynthesis, ChemPhysChem **3**, 243 (2002).

[40] Y. C. Cheng and G. R. Fleming, Dynamics of light harvesting in photosynthesis, Annu. Rev. Phys. Chem. **60**, 241 (2009).

[41] M. B. Plenio, S. F. Huelga, Dephasing-assisted transport: Quantum networks and biomolecules, New J. Phys. **10**, 113019 (2008).

[42] P. Rebentrost, M. Mohseni, I. Kassal, S. Lloyd, and A. Aspuru-Guzik, Environment-assisted quantum transport, New J. Phys. **11**, 033003 (2009).

[43] P. Rebentrost, M. Mohseni, and A. Aspuru-Guzik, Role of quantum coherence and environmental fluctuations in chromophoric energy transport, J. Phys. Chem. B **113**, 9942 (2009).

[44] M. Sarovar and K. B. Whaley, Design principles and fundamental trade-offs in biomimetic light harvesting, New J. Phys. **15**, 013030 (2013).

[45] K. Higgins, S. Benjamin, T. Stace, G. Milburn, B. W. Lovett, and E. Gauger, Superabsorption of light via quantum engineering, Nat. Commun. **5**, 4705 (2014).

[46] G. L. Celardo, F. Borgonovi, M. Merkli, V. I. Tsifrinovich, and G. P. Berman, Superradiance transition in photosynthetic light-harvesting complexes, J. Phys. Chem. C **116**, 22105 (2012).

[47] H. Park, N. Heldman, P. Rebentrost, L. Abbondanza, A. Iagatti, A. Alessi, B. Patrizi, M. Salvalaggio, L. Bussotti, M. Mohseni *et al.*, Enhanced energy transport in genetically engineered excitonic networks, Nat. Mater. **15**, 211 (2016).